

Multi Organ Segmentation of Abdominal Organs Using Cascade Deep Learning Architecture

Bhautik Daxini,^{1*} Dr. M. K. Shah,² Dr. R. K. Shukla³, Rutu Nayak⁴, Ankur Gajjar⁵

Submitted: 07/02/2024 Revised: 15/03/2024 Accepted: 21/03/2024

Abstract: Manual identification of the organs of the body specially the ones located in the abdominal cavity is a tedious work. The accurate segmentation of the abdominal organs is important from the clinical diagnosis and CAD support systems. Recent development in the artificial intelligence have enables us with the cutting edge techniques even for the dense semantic segmentation of medical images. This paper presents a method to automatically segment organs of the abdominal cavity using cascaded V-Net architecture. In this work, the second V-Net is trained with the output of the first stage along with the down sampled original images to provided better contextual details. The model is trained and validated using multi atlas labelling beyond the cranial vault challenge abdomen data set. F1 score of about 90% was achieved for various organs

Keywords: Cascaded V-Net, abdominal organ, segmentation, Deep Learning

INTRODUCTION

Multiple organ segmentation from radiological images is necessary for a variety of clinical applications, including computer-assisted diagnosis and treatment, computer-assisted surgery, and radiation therapy. Due to the low contrast and high variation of shape in computed tomography (CT) images, it appears to be considerably more difficult to segment abdominal organs than it is to segment other inner human tissues such as the brain or the heart¹. The difficulty of segmenting many abdominal organs all at once is examined in this study. The kidneys, liver, and pancreas are some of the organs that fall within this category. Diagnostic interventions, therapy planning, and treatment administration are just few of the many therapeutic activities that can benefit from organ segmentation in abdominal pictures².

Computer-aided diagnosis and biomarker measurement systems require an organ segmentation technique³. In the process of designing radiation treatments, segmentations of treatment volumes and organs-at-risk play an essential role⁴. More generally speaking, surgery planning and delivery can be supported by segmentation-based patient-specific anatomical models using intraoperative image-guidance systems. In a variety of therapeutic contexts, it is of utmost significance to achieve precise segmentation of the abdominal organs using medical pictures. Multi-organ segmentation of abdominal organs using deep learning has gained significant attention in medical imaging research. Within the scope of this research, there is a method based on deep learning for the multi-organ segmentation of abdominal organs.

Abdominal Organs

The organs of the abdomen are those that are located there and serve the portion of the body that is between the thorax (chest) and the pelvis. The digestive system, the metabolic system, and other key physiological activities rely on these organs. The abdominal cavity separates the trunk (the thorax) from the legs (the pelvis)⁵. The diaphragm, in addition to various musculoaponeurotic walls, and the pelvic inlet make up the limits of the abdominal cavity. The abdominal cavity is home to many organs that play important roles in the processes of digestion, elimination of waste, and metabolism. There are nine reference planes, and each quadrant of the abdomen has a different colour. The internal organs of the abdomen are depicted in Figure 1.

¹ Research Scholar, Gujarat Technological University, Ahmedabad (Gujarat), India,² Department of Instrumentation & Control Engineering, Vishwakarma Government Engineering College, Chandkheda, (Gujarat), India,³ Department of Instrumentation & Control Engineering, Government Engineering College, Rajkot (Gujarat), India,⁴ Department of Biomedical Engineering, Government Engineering College, Ghandhinagar, Gujarat, India. ⁵ Department of Instrumentation & Control Engineering, Shantilal Shah Engineering College, Bhavnagar (Gujarat), India

Corresponding Author: Bhautik Daxini, Research Scholar, Gujarat Technological University, Ahmedabad, Gujarat, India

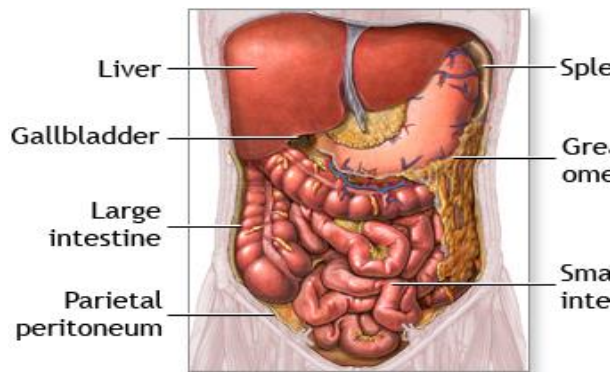


Figure 1. Abdominal Anatomy Organs⁶

The division of this anatomical area into several sections allows for the classification of the locations of the many organs found within the abdominal cavity.

Right Upper Quadrant (RUQ): stomach, pancreas, liver, intestine (duodenum), gallbladder, right kidney, small hepatic flexure.

Right Lower Quadrant (RLQ): small intestine (ileum), cecum, ureter, appendix.

Left Upper Quadrant (LUQ): liver, pancreas, small intestine (jejunum/ileum), spleen, splenic flexure.

Left Lower Quadrant (LLQ): ureter, sigmoid colon. Here is an overview of some major abdominal organs:

Liver:

Detoxification, nutrition metabolism, bile generation, vitamin and mineral storage, and blood clotting protein synthesis are just few of the many jobs performed by the liver, the body's biggest internal organ. It is also essential for the metabolism of carbohydrates, proteins, and lipids⁷.

Stomach:

The digestive process begins in the stomach, a muscular organ that breaks down food. The stomach absorbs food from the esophagus and then secretes gastric fluids, which include enzymes and acid, to help digest the meal. Absorption of certain drugs is also helped along by the stomach⁸.

Pancreas:

The pancreas performs both endocrine and exocrine functions. The enzymes it produces aid in the digestion of both protein and fat in the intestinal tract. Also, it causes the secretion of hormones like insulin and glucagon, which control glucose levels in the blood⁹.

Intestines:

The intestines are divided into the smaller intestine and the larger colon. The small intestine plays a crucial role in the body by absorbing nutrients from digested food. The digestive tract is further subdivided into the duodenum, jejunum, and ileum. The large intestine is responsible for absorbing water from undigested meals and producing stool. The cecal region, colon, rectum, and anus make up this region¹⁰.

Multi-organ segmentation of abdominal organs

The term "multi-organ segmentation of abdominal organs" refers to the process of automatically defining and separating several organs located inside the abdomen area using medical imaging such as CT scans or Magnetic resonance imaging (MRI) scans. This can be done by dividing the abdominal organs into many segments (called "multi-organ segmentation")¹¹. Surgical planning, illness diagnosis, and evaluating the efficacy of a treatment are just a few of the many clinical uses for this work. Several studies have presented distinct algorithms and methodologies for multi-organ segmentation, each making use of a unique combination of machine learning and image processing. Convolutional neural networks (CNNs) and other deep learning models are common method used for multi-organ segmentation¹². These networks can efficiently represent the complicated spatial interactions between different organs because of their ability to autonomously learn hierarchical characteristics from the input pictures. CNN designs including U-Net, V-Net, and 3D variations have been used in several research efforts to address the challenging challenge of multi-organ segmentation. Segmentation is a crucial part of medical image analysis. For many image-processing activities, including visual augmentation¹³, computer-assisted diagnosis and therapies¹⁴, and the extraction of quantitative indicators from pictures, autonomous segmentation of structures and organs of interest is a prerequisite. The capacity to perform volumetric segmentations by taking into account the complete volume content at once is crucial due to the widespread usage of 3D images in diagnostic and interventional imaging.

LITERATURE REVIEW

Many authors have conducted their research in the same direction a literature review and their findings are presented below:

Irshad et al., (2023)¹⁵ proposed a strategy for better abdominal picture segmentation that makes use of organ-boundary prediction as an auxiliary job. The authors employ multi-task learning to train 3D encoder-decoder networks to partition abdominal organs and their borders concurrently. Two network architectures are studied: one in which the tasks share all levels except the task-specific layers, and another in which a single encoder is used for both tasks, but the decoders are kept separate. On two publicly available abdominal CT datasets (Pancreas-CT and Beyond the Cranial Vault (BTCV)), this method is shown to significantly enhance segmentation accuracy, with maximum relative gains of 3.5% and 3.6% in Mean Dice Score for the two datasets, respectively.

Song et al., (2023)¹⁶ presented dynamic loss weighting is a class reweighting approach that gives higher loss weights to organs that are judged to be more difficult to learn based on the available data and the network's current condition to improve the performance

consistency of a segmentation network. The technique uses a second autoencoder to calculate the gap between the network's predictions and the truth, and then uses that information to update its estimate of the loss weight for each organ. This method accurately represents the differences in training difficulty among organs, and it does so in a way that is not sensitive to either data attributes or human biases. Using publicly accessible datasets for abdominal organs and head-neck structures, the system is tested in two multiorgan segmentation tasks, with favourable results from extensive tests demonstrating its validity and efficacy.

Shen et al., (2023)¹⁷ introduced a U-Net-based segmentation model for reliable multi-organ segmentation in abdominal CT images. The key organs for hepato-biliary-pancreatic surgery are highlighted in the model. The model adapts to different backgrounds and organ sizes and shapes by incorporating deformable receptive fields and utilizing information about organ structures. Deformable convolution blocks use trainable offsets to generate suitable receptive fields for shape and size changes, while spatial attention blocks emphasize organ regions of interest. Multi-scale attention maps and semantic knowledge are added to the U-Net's skip-connection architecture. The proposed model is compared against U-Net and its variants in terms of segmentation performance, time required, and model parameters using The Cancer Imaging Archive (TCIA) multi-organ segmentation dataset. The average DICE coefficient for segmentation performance is improved by 80.46 percent using the proposed model, at the expense of an increase of 7.86 percent in model parameters. The proposed model outperforms U-Net on measures of similarity such as DICE, the Jaccard similarity coefficient (JSC), and the Hausdorff distance (HD) by 1.65%, 1.79%, and 4.08%, respectively. Thus, multi-organ segmentation using the suggested model is competitive and promising.

Kaur et al., (2022)¹⁸ examined liver, kidney, and spleen, which are more commonly studied, and instead focusing on the esophagus, duodenum, and portal vein, which are less commonly studied. The magnitude, variety of organ classes, and associated difficulties of datasets are highlighted, highlighting their significance in medical imaging study. The study goes on to describe the qualities of several assessment criteria. The author discussed obstacles and potential solutions and conclude that Dense-Net is the best method for multi-organ segmentation based on the results of the examined studies. The current gold standard employs two-step deep learning models in a sequential fashion, capitalizing on the strengths of both. Overall, this work offers helpful information and direction for future studies.

Kang et al., (2022)¹⁹ emphasized computer-assisted surgery and diagnosis rely heavily on MRI images, highlighting the need of proper segmentation of

abdominal organs. The feature mismatch between shallow and deep features was shown to be a weakness in existing approaches that combine the two in an encoder-decoder framework. The authors incorporated a geographical loss and a semantic loss to bridge the feature gap after quantifying it. Deep characteristics were improved by the spatial loss, whereas shallow features were enriched by the semantic loss. The suggested technique effectively integrated complimentary data from shallow and deep features by constructing and bridging the feature gap. Experiments done on two abdomen MRI datasets showed that the researchers' method greatly outperformed a baseline method with few extra parameters in terms of segmentation performance. The suggested approach excelled at segmenting organs with hazy borders or at low scales, while existing methods struggled.

Jiaqi et al., (2021)²⁰ introduced Computer-aided diagnostic (CAD) systems are offered a fresh strategy for automated abdominal multi-organ segmentation. Using the Simple Linear Iterative Clustering (SLIC) algorithm, the technique extracts super voxels from the pictures whose borders are near anatomical edges, thereby including spatial information into the super voxel classification process. These super voxels have their labels predicted using a random forest classifier, which considers the spatial and intensity properties of the data. The performance of the suggested approach for segmenting the spleen, right kidney, left kidney, and liver area is assessed using thirty abdominal CT images. Experiments show that the suggested strategy improves upon the accuracy of segmentation over the model-based method that was previously used.

Rahul et al., (2021)²¹ presented new deep learning architecture for multi-organ segmentation in abdominal CT images that does not need registration. The suggested technique takes use of U-Net architecture to deal with significant inter-individual variability and adapt to different organs, as opposed to most existing approaches which focus on individual organ segmentation and struggle with shape and position variability. The approach is multi-staged, with each U-Net extensively trained around the organs and building on the input of the preceding step. Superior performance is shown in the evaluation of 50 abdominal CT scans compared to conventional 2D segmentation techniques, with dice/recall/precision/sensitivity values of 99% being achieved for a variety of organs such as the spleen, adrenal glands, gallbladder, kidneys, stomach, aorta, esophagus, veins, liver, inferior vena cava, and pancreas.

Tang et al., (2021)²² introduced automated multi-organ segmentation of 3D abdomen CT scans. The procedure begins with a basic segmentation utilizing a graph partitioning technique, after which spines and ribs are eliminated. The accuracy of the segmentation is enhanced by employing a refinement technique that

makes use of intensity Modeling, a 3D Chan-Vese model, and an organ separation algorithm. A pseudo-3D bottleneck detection technique corrects boundaries. It handles form, location, and weak organ borders effectively. Experimental findings on the XHCSU20 database reveal competitive performance compared to state-of-the-art algorithms, with high Dice similarity coefficients, Jaccard indices, and low liver, spleen, and kidney average symmetric surface distances. The approach also has great organ-specific accuracy, precision, recall, and specificity. SLIVER07 studies also demonstrate its liver segmentation efficiency and accuracy. The suggested technique processes a CT volume in 6 minutes with minimum training and registration.

RESEARCH METHODOLOGY

The concept of designed architecture is examined in the context of research methodology.

Technique Used

There are several techniques used in the proposed methodology. These techniques are given below:

Deep Learning (DL)

DL is a branch of Machine Learning (ML) within the broader area of Artificial Intelligence (AI). The representation of data at various levels of abstraction could be accomplished in DL via the use of many layers of abstraction. Despite the significant strides that have been achieved in the field of computer science thanks to deep learning, identifying, and classifying medical pictures remains a significant challenge. A recent development in copy-move forgeries is the tendency toward improved medical image understanding. The identification and classification of pictures are two of the most essential applications that could be accomplished using deep learning. It does this by taking the data straight from the two-dimensional photos and then automatically learning from the information that the conventional hand-held extraction techniques provide. This helps it to avoid a range of inaccuracies that could occur. The error is calculated at the backpropagation stage of equation 1, which is the first step^{23,24}.

$$\frac{\partial E}{\partial W_{ab}} = \sum_{i=0}^{N-m} \sum_{j=0}^{N-m} \frac{\partial E}{\partial W_{ij}^1} \frac{\partial x_{ij}^1}{\partial W_{ab}} \sum_{i=0}^{N-m} \sum_{j=0}^{N-m} \frac{\partial E}{\partial W_{ij}^1} y(i + a)(j + b)^{l-1}$$

(1)

Here, E denotes the error function, x denotes the input, and y is the output. i^{th} , j^{th} and m^{th} are filter size, N denotes the number of particles in each layer, l represents layer number, and W denotes filter weight with a and b indices. There are several hidden layers in the structure of deep learning that analyze incoming data as seen in figure 2.

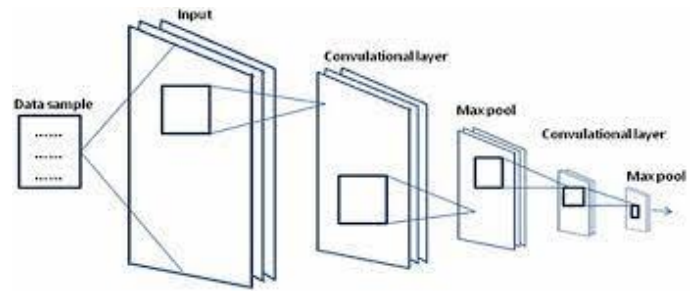


Figure 2. Deep Learning [24].

V-Net

V-Net, short for Volumetric Neural Network, is a deep learning architecture designed for 3D image segmentation tasks. V-Net's primary use is in medical imaging, where it is used to identify and isolate anatomical features from volumetric medical data like CT and MRI images. The design takes advantage of fully convolutional neural networks (FCNs) to handle 3D volumes quickly, enabling precise and in-depth segmentation of organs, tissues, or anomalies. Segmentation is a crucial part of medical image analysis²⁵. Figure 3 illustrates the architecture of V-Net.

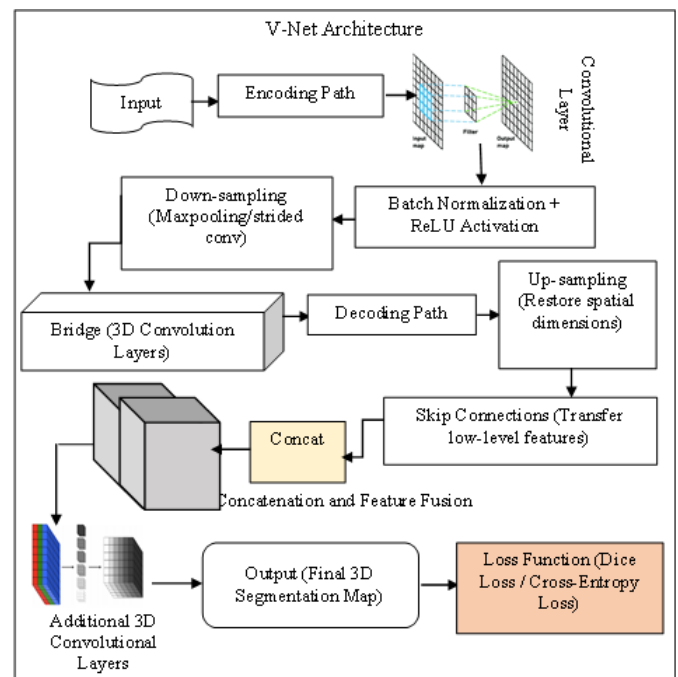


Figure 3. V-Net Architecture

Automated organ and structure detection and segmentation is frequently required for applications including visual augmentation, computer-assisted diagnosis and intervention, and the extraction of quantitative indicators from pictures²⁶. The V-Net architecture can be mathematically represented as $Y = D(E(X))$, where X is the input volume, E is the encoding function, D is the decoding function, and Y is the segmented output. The network learns the appropriate

parameters during training to optimize the segmentation performance based on labelled training data.

Cascaded Network

The cascaded network where the training images serves as the input to the first stage of the network. The first stage is optimized using a loss function. The output of the first stage along with the processed input images serves as the input to the second stage of the network, which is optimized by another loss function. This type of network has shown better performance as compared to single stage architecture.²⁷

Windowing

Windowing, also referred to as grey-level visualisation, is the exploitation of the CT image greyscale component through CT numbers to alter the image's appearance and prioritise specific structures. The image's brightness as well as contrast both are varied by changing level and width of the window respectively. The density of various tissues of the body are measure in Hounsfield Unit (HU). The organ of the abdominal cavity are having very similar as all are made up of soft tissues, so it is suggested that the organs having similar tissues, the window of narrow size should be used. This is because any minute changes in the details will be amplified over the entire grey scale range. A soft tissue window range except for lungs is given with as, level: +50 HU; Width: 350 HU (Range: -125 to +225)^{28,29}

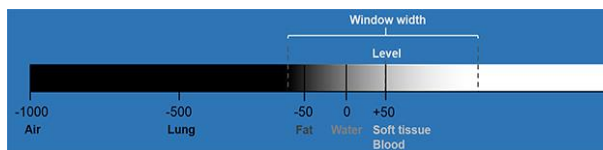


Figure 4. HU scale for soft organ²⁹

METHOD

This section describes the datasets, pre-processing, segmentation process, hardware specification and performance assessment measures.

Data Set

The dataset is from Multi-Atlas Labeling Beyond the Cranial Vault - Workshop and Challenge, with project storage location as synapse storage and project SynID as syn3193805³⁰. It basically consists of 2 data set, one of abdomen and another of cervical. The abdomen data set consisting of 30 training sets has been used for the training of the model. The 20 test data were not available as it was a part of challenge.

Pre-processing

The pre-processing techniques that were employed were alignment, augmentation, normalization, clipping voxel intensities. First the CT scans were aligned to be in the same orientation. Utilising normalisation in a model enhances the speed of learning and promotes stability in gradient descent. The axial spacing was normalized to 3mm and HU values were truncated between [-250,250]

HU. Only the slice containing the organ is used for the training the model.

Segmentation

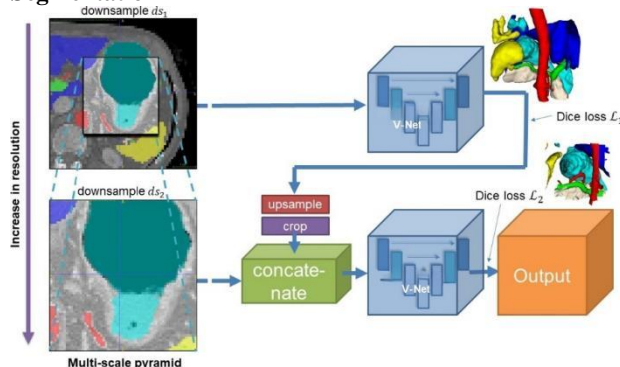


Figure 5. Cascaded V-Net

As shown in Figure 5, cascaded V-Net is employed for the segmentation of the input images. The V-Net is trained in the initial stage utilising low-resolution images to capture extensive context, down sampled by a certain factor, then optimised with the Dice loss function. In the following stage, we incorporate the forecasted segmentation maps as an additional input channel into the V-Net. We train the model on images at a higher resolution, which have been reduced in size by a specific factor, and optimise it using Dice loss. The input for this second level of the pyramid involves up sampling the prediction maps from the previous level by a factor of 2 and cropping them to align geographically with the higher resolution layers. These predictions can be combined with the properly cropped image data as a secondary channel. Each stage consists of 4 decoder stages, 4 encoder stages and one concatenation stage. The original 5x5x5 convolution kernel is replaced with 3x3x3. Dropout was employed except for the first and last stage. A total of 9,332,094 trainable parameters, about 9.3 million in each stage. Total of about 18 million parameters

Conceptually each V-Net block can be represented as follows.

Let V be the V-Net architecture used for multi-organ segmentation.

Let \hat{Y} be the segmented images produced by V using the training set X_{train}

$$\hat{Y} = V(X_{train}) \quad (2)$$

Let Θ be the set of parameters of the V-Net model V .

Let L be the chosen loss function for segmentation, and O be the selected optimizer and θ^* be the trained parameters. θ_{final} be the final set of trained and fine tuned parameters.

The training process aims to minimize the loss over the training set in each stage:

$$\theta^* = \operatorname{argmin}_{\theta} (\sum_{(x_i, y_i) \in X_{train}} L(V(x_i; \theta), y_i)) \quad (3)$$

$$\theta^* = \text{Train}(V, X_{\text{train}}, L, O) \quad (4)$$

The model is then validated through fine tuning using the validation dataset.

$X_{\text{validation}}$ and adjusting θ^* based on the result.

$$\Theta_{\text{fine-tuned}} = \text{FineTune}(\theta^*, X_{\text{validation}}, L, O) \quad (5)$$

Adam, AdamW, RMSprop optimizer were used and the initial learning rate was set to $1e-4$ and batch size was set to 3.

Hardware

The hardware configuration used for training the model is given below.

Table1: Hardware configuration

Graphic Card	INNO3D GRAPHIC CARD RTX3060 12GB DDR6
RAM	CORSIER RAM 64 GB DDR-5 5200MHZ
CPU	INTEL CORE-I9 12900K
Mother Board	GIGABYTE Z790 UD AC MOTHER BOARD
Hard Disk	WD 2 TB SATA HDD, WD 250 GB SATA HDD

Performance Assessment Measure

Loss function used for evaluation of performance is Dice coefficient or F1 score. Mean dice loss was calculated and compared for various epoch and optimizers.

$$\begin{aligned} \text{Dice Score} &= \frac{2 * |A \cap B|}{2 * |A \cap B| + \frac{|B|}{|A|} + \frac{|A|}{|B|}} \\ &= \frac{2 * |A \cap B|}{|A| + |B|} \quad (6) \end{aligned}$$

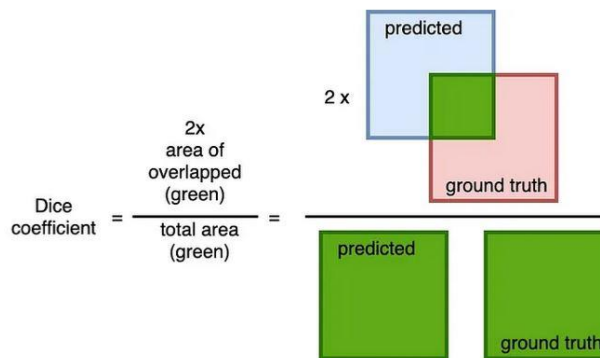


Figure 6: Dice Loss

RESULT

The model was tested for various epochs for Adam optimizer and the average dice loss was compared. The model performance was also compared for different optimizers at 1000 epochs.

1) With optimizer = Adam, learning rate = $1e-4$, Activation function= ReLu. Dataset = synapse, No of epochs = 50

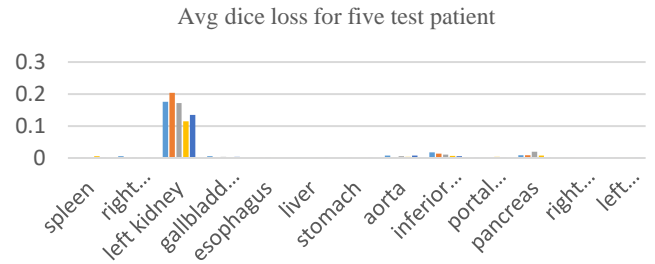


Figure 7: Avg. dice loss for five test patient after 50 epochs & Adam optimizer

2) With optimizer = Adam, learning rate = $1e-4$, Activation function= ReLu. Dataset = synapse, No of epochs = 100

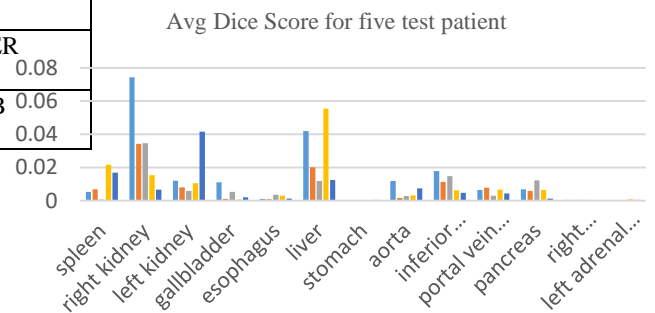


Figure 8: Avg. dice loss for five test patient after 100 epochs & Adam optimizer

3) With optimizer = Adam, learning rate = $1e-4$, Activation function= ReLu. Dataset = synapse, No of epochs = 500

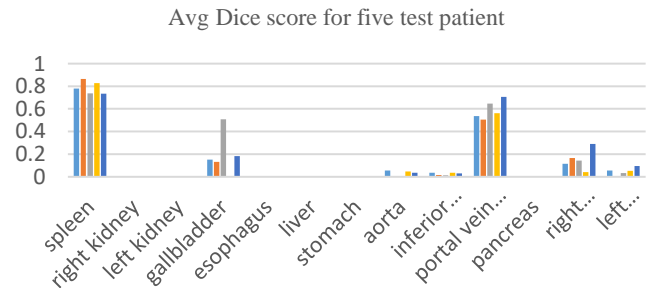


Figure 9: Avg. dice loss for five test patient after 500 epochs & Adam optimizer

4) With optimizer = Adam, learning rate = $1e-4$, Activation function= ReLu. Dataset = synapse, No of epochs = 1000

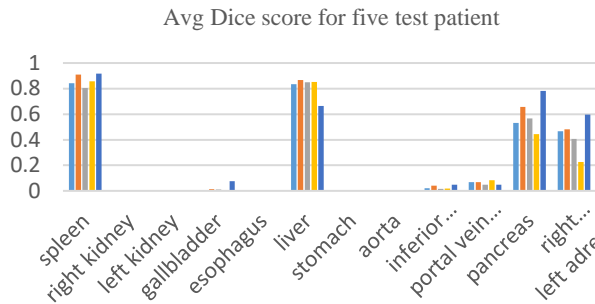


Figure 10: Avg. dice loss for five test patient after 1000 epochs & Adam optimizer

5) With optimizer = Adam, learning rate = $1e-4$, Activation function= ReLu. Dataset = synapse, No of epochs = 2000

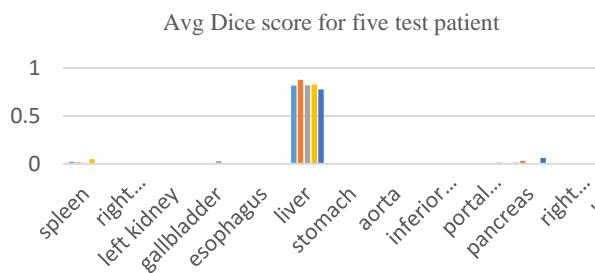


Figure 11: Avg. dice loss for five test patient after 2000 epochs & Adam optimizer

6) With optimizer = Adam, learning rate = $1e-4$, Activation function= ReLu. Dataset = synapse, No of epochs = 3000

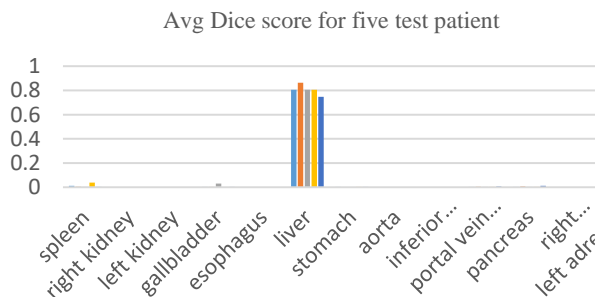


Figure 12: Avg. dice loss for five test patient after 3000 epochs & Adam optimizer

7) With optimizer = AdamW, learning rate = $1e-4$, Activation function= ReLu. Dataset = synapse, No of epochs = 1000

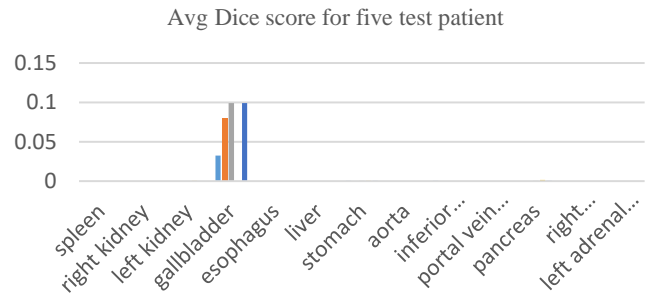


Figure 13: Avg. dice loss for five test patient after 1000 epochs & AdamW optimizer

8) With optimizer = RMSprop, learning rate = $1e-4$, Activation function= ReLu. Dataset = synapse, No of epochs = 1000

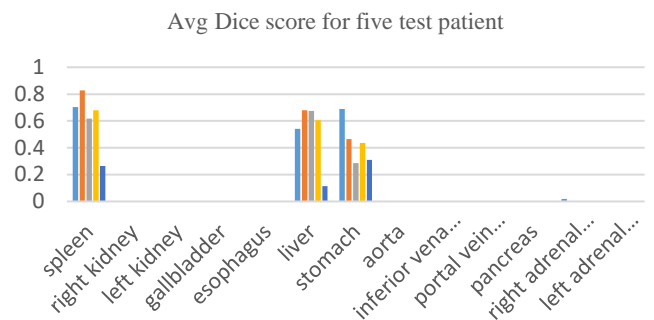


Figure 14: Avg. dice loss for five test patient after 1000 epochs & RMSprop optimizer

The standard HU values for various organs are given in the following table.

Table 2: Standard HU values for some of the abdominal organs

Organ	Standard HU values	Reference
Liver	60 +/- 6	31.
Kidney	+20 to +45	31.
Gall Bladder	0 to 20	32.
Pancreas	30 to 50	33.
Spleen	40 to 60	34.

CONCLUSION

Referring table 2 and the outputs of the model w.r.t. different optimizer and for different epochs the following points were observed.

- For the same number of epochs, for different optimizers, the model was able to segment different abdominal organs.
- For the Adam optimizer as the number of epochs increases, different abdominal organs were segmented. The organs having HU range on the lower side were segmented for less number of epochs. As the number of epochs increased, the organs with higher HU range were segmented by the model.
- The performance of AdamW optimizer was worst as compared to Adam and RMSprop.

- The model converges with increases in epochs resulting in decrease of mean dice loss however the convergence requires a large number of epochs and time.
- The training of segmentation models is a memory hungry process, requiring a huge amount of memory and more amount of stagnant time for training.

REFERENCES

- [1] Zhou, Yuyin, Yan Wang, Peng Tang, Song Bai, Wei Shen, Elliot Fishman, and Alan Yuille. "Semi-supervised 3D abdominal multi-organ segmentation via deep multi-planar co-training." In 2019 IEEE Winter Conference on Applications of Computer Vision (WACV), pp. 121-140. IEEE, 2019.
- [2] Liu, Yiqiao, Madhu Gargasha, Mohammed Qutaish, Zhuxian Zhou, Bryan Scott, Hamed Yousefi, Zhengrong Lu, and David L. Wilson. "Deep learning based multi-organ segmentation and metastases segmentation in whole mouse body and the cryo-imaging cancer imaging and therapy analysis platform (CITAP)." In *Medical Imaging 2020: Biomedical Applications in Molecular, Structural, and Functional Imaging*, vol. 11317, pp. 215-225. SPIE, 2020.
- [3] Gibson, Eli, Francesco Giganti, Yipeng Hu, Ester Bonmati, Steve Bandula, Kurinchi Gurusamy, Brian Davidson, Stephen P. Pereira, Matthew J. Clarkson, and Dean C. Barratt. "Automatic multi-organ segmentation on abdominal CT with dense V-networks." *IEEE transactions on medical imaging* 37, no. 8 (2018): 1822-1834.
- [4] Sykes, Jonathan. "Reflections on the current status of commercial automated segmentation systems in clinical practice." *Journal of medical radiation sciences* 61, no. 3 (2014): 131-134.
- [5] Weinstein, Adam L., and Alaa Abd-Elseyed. "Abdominal Anatomy." *Pain: A Review Guide* (2019): 803-805.
- [6] <https://slu.adam.com/content.aspx?productid=117&pid=2&gid=8896>
- [7] Garbar, Veronica, and Bruce W. Newton. "Anatomy, abdomen and pelvis, falciform ligament." (2019).
- [8] Konturek, S. J., P. C. Konturek, Tomasz Brzozowski, and G. A. Bubenik. "Role of melatonin in upper gastrointestinal tract." *Journal of physiology and pharmacology* 58, no. 6 (2007): 23-52.
- [9] Bakhti, Mostafa, Anika Böttcher, and Heiko Lickert. "Modelling the endocrine pancreas in health and disease." *Nature Reviews Endocrinology* 15, no. 3 (2019): 155-171.
- [10] Johansson, Malin EV, and Gunnar C. Hansson. "Immunological aspects of intestinal mucus and mucins." *Nature Reviews Immunology* 16, no. 10 (2016): 639-649.
- [11] Avendi, Michael R., Arash Kheradvar, and Hamid Jafarkhani. "A combined deep-learning and deformable-model approach to fully automatic segmentation of the left ventricle in cardiac MRI." *Medical image analysis* 30 (2016): 108-119.
- [12] Milletari, Fausto, Nassir Navab, and Seyed-Ahmad Ahmadi. "V-net: Fully convolutional neural networks for volumetric medical image segmentation." In 2016 fourth international conference on 3D vision (3DV), pp. 565-571. Ieee, 2016.
- [13] Bernard, Olivier, Johan G. Bosch, Brecht Heyde, Martino Alessandrini, Daniel Barbosa, Sorina Camarasu-Pop, Frederic Cervenansky et al. "Standardized evaluation system for left ventricular segmentation algorithms in 3D echocardiography." *IEEE transactions on medical imaging* 35, no. 4 (2015): 967-977.
- [14] Zettinig, Oliver, Amit Shah, Christoph Hennemersperger, Matthias Eiber, Christine Kroll, Hubert Kübler, Tobias Maurer et al. "Multimodal image-guided prostate fusion biopsy based on automatic deformable registration." *International journal of computer assisted radiology and surgery* 10 (2015): 1997-2007.
- [15] Irshad, S., Gomes, D. P., & Kim, S. T. (2023). Improved abdominal multi-organ segmentation via 3D boundary-constrained deep neural networks. *IEEE Access*, 11, 35097-35110.
- [16] Song, Youyi, Jeremy Yuen-Chun Teoh, Kup-Sze Choi, and Jing Qin. "Dynamic Loss Weighting for Multiorgan Segmentation in Medical Images." *IEEE Transactions on Neural Networks and Learning Systems* (2023).
- [17] Shen, Nanyan, Ziyang Wang, Jing Li, Huayu Gao, Wei Lu, Peng Hu, and Lanyun Feng. "Multi-organ segmentation network for abdominal CT images based on spatial attention and deformable convolution." *Expert Systems with Applications* 211 (2023): 118625.
- [18] Kaur, Harinder, Navjot Kaur, and Nirvair Neeru. "Evolution of multiorgan segmentation techniques from traditional to deep learning in abdominal CT images—A systematic review." *Displays* 73 (2022): 102223.
- [19] Kang, Susu, Muyuan Yang, X. Sharon Qi, Jun Jiang, and Shan Tan. "Bridging Feature Gaps to Improve Multi-Organ Segmentation on Abdominal Magnetic Resonance Image." *IEEE Journal of Biomedical and Health Informatics* 27, no. 3 (2022): 1477-1487.
- [20] Wu, Jiaqi, Guangxu Li, Huimin Lu, and Tohru Kamiya. "A supervoxel classification-based method for multi-organ segmentation from abdominal ct

- images." *Journal of Image and Graphics* 9, no. 1 (2021): 9-14.
- [21] Jain, Rahul, Anoushka Sutradhar, Amiya K. Dash, and Suchismita Das. "Automatic Multi-organ Segmentation on Abdominal CT scans using Deep U-Net Model." In *2021 19th OITS International Conference on Information Technology (OCIT)*, pp. 48-53. IEEE, 2021.
- [22] Tang, Ping, Yu-qian Zhao, and Miao Liao. "Automatic multi-organ segmentation from abdominal CT volumes with LLE-based graph partitioning and 3D Chan-Vese model." *Computers in Biology and Medicine* 139 (2021): 105030.
- [23] Wang, Guotai, Wenqi Li, Maria A. Zuluaga, Rosalind Pratt, Premal A. Patel, Michael Aertsen, Tom Doel et al. "Interactive medical image segmentation using deep learning with image-specific fine tuning." *IEEE transactions on medical imaging* 37, no. 7 (2018): 1562-1573
- [24] <https://medium.com/@singole/an-extensive-guide-to-convolution-neural-network-2023-84872b16bd78>
- [25] Milletari, Fausto, Nassir Navab, and Seyed-Ahmad Ahmadi. "V-net: Fully convolutional neural networks for volumetric medical image segmentation." In *2016 fourth international conference on 3D vision (3DV)*, pp. 565-571. Ieee, 2016.
- [26] Bernard, Olivier, Johan G. Bosch, Brecht Heyde, Martino Alessandrini, Daniel Barbosa, Sorina Camarasu-Pop, Frederic Cervenansky et al. "Standardized evaluation system for left ventricular segmentation algorithms in 3D echocardiography." *IEEE transactions on medical imaging* 35, no. 4 (2015): 967-977.
- [27] Roth, H.R. et al. (2018). A Multi-scale Pyramid of 3D Fully Convolutional Networks for Abdominal Multi-organ Segmentation. In: Frangi, A., Schnabel, J., Davatzikos, C., Alberola-López, C., Fichtinger, G. (eds) *Medical Image Computing and Computer Assisted Intervention – MICCAI 2018*. MICCAI 2018. *Lecture Notes in Computer Science()*, vol 11073. Springer, Cham.
- [28] <https://www.sciencedirect.com/topics/medicine-and-dentistry/hounsfield-scale>
- [29] <https://www.kaggle.com/code/redwankarimsony/ct-scans-dicom-files-windowing-explained>
- [30] <https://www.synapse.org/#!Synapse:syn3193805/wiki/217752>
- [31] https://en.wikipedia.org/wiki/Hounsfield_scale
- [32] Havrilla TR, Reich NE, Haaga JR, Seidelmann FE, Cooperman AM, Alfydi RJ. Computed tomography of the gallbladder. *AJR Am J Roentgenol*. 1978 Jun;130(6):1059-67. doi: 10.2214/ajr.130.6.1059. PMID: 418641.
- [33] <https://emedicine.medscape.com/article/371613-overview>
- [34] <https://www.ncbi.nlm.nih.gov/books/NBK554559>